C-
30/6/89

Hydraulics Research
Wallingford

AN INVESTIGATION OF PARTIALLY REFLECTING BOUNDARY CONDITIONS FOR A NON-LINEAR NUMERICAL MODEL OF WAVE DISTURBANCE

D V Jones BSc PhD
J V Smallman BSc PhD

Report No SR 185
November 1988

Registered Office: Hydraulics Research Limited,
Wallingford, Oxfordshire OX10 8BA.
Telephone: 0491 35381. Telex: 848552

This report describes work supported under contract PECD 7/6/053 funded by the Department of the Environment. The DOE nominated officer was Dr R Thorogood. Dr S W Huntington was Hydraulics Research's nominated officer. The report is published with the permission of the Department of the Environment but any opinions expressed are not necessarily those of the funding department.

An investigation of partially reflecting boundary conditions for a non-linear numerical model of wave disturbance.
D V Jones and J V Smallman, Report No SR 185, November 1988

ABSTRACT

This report describes the further development of a finite difference model which solves the Boussinesq equations in water of variable depth. The main objective of the work reported here was to examine methods for representing partially reflecting boundaries in the existing model.

The first stage in this work was to examine the methods available for representing partially reflecting boundaries. These were reviewed and their relative merits assessed. This indicated that a good approach would be to further investigate the use of sponge layer boundary conditions. These are used with some success in the numerical model to represent fully absorbing boundaries. To do this required both a fuller understanding and development of the theoretical basis of sponge layers.

The theory of sponge layers is described in some detail in this report, prior to extending it to allow for partially reflecting boundaries. The theory was then implemented in the numerical model and a series of tests conducted to examine the performance of the boundary conditions. It was found that good agreement was achieved both with theoretically determined reflection coefficients, and with results from a limited physical model data set.

The work described here provides a good basis for further development of this approach to represent the reflection properties of physically realistic structures in harbour wave disturbance models.

CONTENTS

1 INTRODUCTION

1.1 Background

A numerical model has already been developed for the solution of the Boussinesq equations for shallow water waves. This model describes well the physical processes of diffraction and refraction of nonlinear dispersive wave propagation (Refs 1 and 2), and includes numerical boundary conditions that successfully model both total reflection and total absorption. Absorption is achieved using a sponge layer, as developed by Larsen and Dancy (Ref 3). However, in order to model the reflective behaviour of real harbour boundaries, which may vary from vertical walls through rubble mound structures to gently sloping beaches, a new approach is required. It is also important to represent the reflection characteristics of real boundaries throughout the frequency component range of a random sea.

1.2 Review of recent literature

The most common analytical approach to the problem of representing outgoing boundaries, is to use radiation boundary conditions. Israeli and Orszag (Ref 4) have summarised methods of deriving higher order approximations to radiation boundary conditions, and Chubarov and Shokin (Ref 5) have considered the discretisation of such methods, with particular reference to nonlinearity and dispersion. Recent work in this area for the shallow water equations has been completed by Burgess (Ref 6). However, these methods are generally derived assuming normally incident waves and are less accurate for obliquely incident waves. They also require finite differencing of higher order terms.

An attractive approach to radiation boundary conditions developed by Liao and Wang (Ref 7), which uses an extrapolation series, is accurate for oblique incidence. It seems likely that this method could be modified to represent partially reflecting boundaries, but has the drawback of needing information at several previous time levels.

The governing equations of porous media have been used quite successfully (eg Madsen (Ref 8)) to represent both reflecting and transmitting boundaries. This method requires the empirical tuning of several constants in the equations. However, it is not clear if these equations are applicable to rubble structures.

The existing absorbing boundary conditions used in the Hydraulics Research numerical model (Ref 1) are based on the work of Larsen and Dancy (Ref 3). They employ a sponge layer, which is used to absorb the energy of waves incident upon it. When used in this way the sponge layer can be thought of as acting in the same way as a shingle beach in a physical model of wave disturbance, in that it will absorb waves over a wide range of frequencies. In the derivation of the sponge layer representation the aim is to select certain parameters so as to minimise the reflection coefficient of the boundary. It seems equally possible that a form of sponge layer could be obtained which would behave physically like a partially reflecting structure. As far as is known no previous workers have made attempts to control a sponge layer to represent a partially reflecting boundary.

1.3 Outline of approach

The method finally chosen is based on the sponge layer approach of Ref 3, with the aim of increasing the reflection coefficient from the present absorbing case to give partial reflection. In common with the porous media layer, it was anticipated that the sponge layer would perform well throughout the frequency range of interest, with the advantage of being easier to implement than the porous media layer.

In order to control the sponge layer reflection coefficient, it is necessary to derive the governing equations inside the sponge layer, from the finite difference expressions within the sponge. The requirement of continuity across the sponge boundary then gives the theoretical reflection coefficient. This analysis is necessarily linear, which is also the case when analysing the porous media layer (Ref 9). The derivation of the theoretical reflection coefficient for the sponge layer is given in Chapter 2.

Prior to this some consideration is given to alternative formulations of the model boundary conditions. This is also discussed in Chapter 2. Numerical tests have been conducted to check the accuracy and applicability of the sponge layer theory, and these are detailed in Chapter 3. The conclusions and recommendations arising from this research are given in Chapter 4.

2 THEORETICAL BACKGROUND

2.1 Alternative boundary conditions

Before the introduction of a sponge layer, the present numerical model used an absorbing boundary condition. This was based on the characteristic equation of the one dimensional, linear shallow water equation:

$$\frac{dx}{dt} = \pm\ (gh)^{\frac{1}{2}} \qquad (2.1)$$

where x is distance, t is time and h is water depth. By assuming that the wave propagation obeys equation (2.1), a linear condition can be imposed at the boundary based on the information one cell before it. This boundary condition can be tuned to a specific frequency and direction, and will work well for the given case. However, as incident waves deviate from their assumed behaviour the boundary condition will become less effective and wave energy will be reflected. Where this type of boundary condition has been set up for short period waves a significant fraction of the long period energy (eg in the case of set down) will be reflected, see Smallman et al (Ref 1).

An improvement might be expected with the non-linear characteristic equation which for the right-going wave is:

$$\frac{dx}{dt} = u + (gh)^{\frac{1}{2}} \qquad (2.2)$$

A finite difference expression based on equation (2.2), which uses linear interpolation across the cell before the boundary, is

$$u_{i+1}^{n+1/2} = u_{i+1}^{n-1/2} - (\bar{u} + (g\bar{h})^{1/2})\frac{\Delta t}{\Delta x}\ (u_{i+1}^{n-1/2} - u_i^{n-1/2}) \tag{2.3}$$

where space level i+1 corresponds to the boundary. $\bar{u}$ and $\bar{h}$ are mean values of u and h respectively over the fraction of the last cell covered by the wave in time Δt. A simple approximation to $\bar{u}$ and $\bar{h}$ would be:

$$\begin{aligned} \bar{u} &= 1/2(u_i^{n-1/2} + u_{i+1}^{n+1/2}) \\ \bar{h} &= z_{i+1/2}^{n} + 1/2(d_i + d_{i+1}) \end{aligned} \tag{2.4}$$

where d_i is the still water depth at the ith cell.

Numerical tests using this non-linear boundary condition for the Boussinesq equations, showed that although it was a more effective absorber than the previous linear boundary condition, it was still unsatisfactory.

Two obvious inadequacies of the non-linear boundary condition are its failure to take into account the slowing of the wave due to dispersion, and the linear interpolation and approximations made in deriving equations (2.3) and (2.4). Unfortunately a characteristics-based analysis of the dispersive Boussinesq equations is presently intractable, so preventing the derivation of an extension to equations (2.1) and (2.2). An attempt to approximate the effect of dispersion, using the equation:

$$\frac{dx}{dt} = \frac{u + (gh)^{1/2}}{(1 + k^2h^2/3)^{3/2}} \tag{2.5}$$

did not improve the effectiveness of the boundary condition. Efforts to improve the interpolation and approximations of equations (2.3) and (2.4), by using slightly more sophisticated expressions, also had a negligible effect.

A further drawback of the absorbing boundary condition approach as described above, is revealed when attempts are made to apply the method to partial reflection. As an example, the linear boundary condition based on equation (2.1) can be written as:

$$u_{i+1}^{n+\frac{1}{2}} = (1-R)\ [u_{i+1}^{n-\frac{1}{2}} + (u_{i}^{n-\frac{1}{2}} - u_{i+1}^{n-\frac{1}{2}})c\ \Delta t/\Delta x] \qquad (2.6)$$

where c is the celerity. R = 1 gives zero velocity at the boundary, corresponding to total reflection, and R = 0 gives total absorbtion. Numerical tests have confirmed that for an incident sine wave, these two values of R give very good results. However, as R varied between 0 and 1, numerical tests showed that even for incident sine waves, the effective reflection coefficient was period dependent, and not in general close in value to R. Equation (2.6) is therefore unreliable for values of R other than 0 or 1, even for incident sine waves. This suggests that even if a perfectly absorbing boundary condition could be found for non-linear, dispersive waves, it would be difficult to control it in the case of partial reflection.

2.2 Analysis of the sponge layer reflection coefficient

Before discussing a method by which the sponge layer can be used to represent a partially reflecting boundary, some background should be given on sponge layers as absorbing boundary conditions. The basic idea behind sponge layers is that in the cells representing an absorbing boundary the wave elevation and velocity are reduced by successive division by a function $\mu(x)$ (say). This is selected so that it is equal to one at the front of the layer and has a large value at the back. Thus the wave energy is dissipated as it travels through the layer in a similar way in which it would be by a gently sloping beach. The reflection behaviour of the sponge layer is directly related to the choice of the function μ and the number of model cells over which it is applied. The expected reflection behaviour is derived from the finite difference scheme. In the following section a method of analysis will be used which is similar to that given in Larsen and Dancy (Ref 3).

For simplicity, we consider the one dimensional linearised shallow water equations:

$$\frac{\partial t}{\partial t} + d\,\frac{\partial u}{\partial x} = 0 \qquad (2.7)$$

$$\frac{\partial u}{\partial t} + g\,\frac{\partial z}{\partial x} = 0 \qquad (2.8)$$

The sponge function μ(x) has been introduced in a previous report (Ref 1). There, it was used once, at the end of the finite difference scheme, to progressively reduce elevations and velocities towards the boundaries. The scheme used in the present model is a predicter-corrector and calculates the elevations before the velocities. We will now change the application of the sponge, so that the elevations are affected before calculating the velocities. This is equivalent to the following scheme:

$$\frac{1}{\Delta t}\left(z^{n+1}_{i-\frac{1}{2}} - \frac{z^{n}_{i-\frac{1}{2}}}{\mu_{i-\frac{1}{2}}}\right) + \frac{d}{\Delta x}\left(\frac{u^{n+\frac{1}{2}}_{i}}{\mu_{i}} - \frac{u^{n+\frac{1}{2}}_{i-1}}{\mu_{i-1}}\right) = 0 \qquad (2.9)$$

$$\frac{1}{\Delta t}\left(u^{n+3/2}_{i} - \frac{z^{n+\frac{1}{2}}_{i}}{\mu_{i}}\right) + \frac{g}{\Delta x}\left(\frac{z^{n+1}_{i+\frac{1}{2}}}{\mu_{i+\frac{1}{2}}} - \frac{z^{n+1}_{i-\frac{1}{2}}}{\mu_{i-\frac{1}{2}}}\right) = 0 \qquad (2.10)$$

in the usual notation.

This double application of the sponge is necessary to give equations (2.9) and (2.10) a similar form, which will be useful in the later analysis.

To derive the theoretical reflection coefficient we first need to re-arrange equation (2.9) as:

$$\frac{1}{\Delta t}\left(z_{i-\frac{1}{2}}^{n+1} - z_{i-\frac{1}{2}}^{n}\right) + \frac{d}{\Delta x}\left(\frac{u_i^{n+\frac{1}{2}}}{\mu_i} - \frac{u_{i-1}^{n+\frac{1}{2}}}{\mu_{i-1}}\right) = \frac{z_{i-\frac{1}{2}}^{n}}{\Delta t}\left(\frac{1}{\mu_{i-\frac{1}{2}}} - 1\right) \tag{2.9a}$$

Making the approximation that the RHS of this equation is centred at the time level $(n+\frac{1}{2})\Delta t$, which will introduce an error which increases with increasing time step, we can write the differential equation corresponding to (2.9a) as:

$$\frac{\partial z}{\partial t} + d\,\frac{\partial}{\partial x}(u/\mu) = \frac{z}{\Delta t}\left(\frac{1}{\mu} - 1\right) \tag{2.11}$$

Likewise equation (2.10) gives (with the same approximation)

$$\frac{\partial u}{\partial t} + g\,\frac{\partial}{\partial x}(z/\mu) = \frac{u}{\Delta t}\left(\frac{1}{\mu} - 1\right) \tag{2.12}$$

Now making the substitutions, (assuming harmonic motion)

$$z = \frac{z^*(x)}{g^{\frac{1}{2}}}\,\mu e^{iwt} \quad ; \quad u = \frac{u^*(x)}{d^{\frac{1}{2}}}\,\mu e^{iewt} \tag{2.13}$$

lead to the equations

$$\frac{du^*}{dx} = -\gamma z^* \tag{2.14}$$

$$\frac{dz^*}{dx} = -\gamma u^* \tag{2.15}$$

$$\text{where } k = \frac{w}{(gd)^{½}} \quad , \quad C_r = (gd)^{½} \frac{\Delta t}{\Delta x} \tag{2.16}$$

$$\text{and} \quad \gamma(x) = \{ik - \frac{(\mu^{-1} - 1)}{C_r \Delta x}\} \mu(x) \tag{2.17}$$

Equation (2.17) can be compared with equation 14 of Ref 3. There, Larsen and Dancy used a Preissman Box scheme, involving three time levels, which replaces μ^{-1} in equation (2.17) here by μ^{-2}. This complicates the expression, and makes the subsequent integration of $\gamma(x)$ more difficult. Equations (2.14) and (2.15) give

$$\frac{d^2z^*}{dx^2} - \left(\frac{1}{\gamma}\frac{d\gamma}{dx}\right)\frac{dz^*}{dx} + \gamma^2 z^* = 0 \tag{2.18}$$

with a similar equation for u*. Although no general method is known for the solution of a second order linear ordinary differential equation with variable coefficients, equation (2.18) is of a special type, with a solution of the form:

$$z_s^*(x) = A\left\{e^{\int_x^{x_e} \gamma(s)ds} - e^{-\int_x^{x_e} \gamma(s)ds}\right\} \tag{2.19}$$

$x_s \le x \le x_e$. Here the sponge layer acts on the region $x_s \le x \le x_e$, A is a constant, and the solution requires zero elevation at the back of the sponge layer (at the boundary). Note that in the discrete application of this boundary condition, a slight error will be introduced, because the elevation will be zero at the centre of a cell, not at the back. This will decrease as Δx decreases.

If we now define $f(x) = \int_{x}^{x_e} \gamma(s)ds$ (2.20)

then (2.19) becomes

$$z_s^* = B\sinh f(x) \tag{2.21}$$

where B is a constant.

At the start of the sponge layer, the governing equations change from equations (2.7) and (2.8) to equations (2.11) and (2.12). Continuity of the solution is required across this interface; the boundary condition is

$$\frac{\partial z}{\partial x} + akz = 0 \quad \text{on } x = x_s, \tag{2.22}$$

where a is a complex reflection coefficient (see, for example, Berkhoff (Ref 10)).

Outside the sponge, the solution can be written

$$z = e^{-ikx} + Re^{ikx} \tag{2.23}$$

which corresponds to a unit amplitude right going wave and its reflection of amplitude R.

Substituting equation (2.23) and its differential into equation (2.22) allows an expression for the amplitude of the reflection coefficient to be derived as:

$$R = \left(\frac{ik - ak}{ik + ak}\right)\Bigg|_{x=x_s} e^{-2ikx_s} \tag{2.24}$$

From equation (2.22), $ak = -\frac{1}{z}\frac{dz}{dx}$ and thus

$$R = \left(\frac{ikz + dz/dx}{ikz - dz/dx}\right)\Bigg|_{x=x_s} e^{-2ikx_s} \tag{2.25}$$

Now in the sponge, from equation (2.13),

$$z = \frac{z_s^*(x)}{g^{1/2}} \mu(x)\ e^{iwt}$$

and therefore

$$\frac{dz}{dx} = \frac{e^{iwt}}{g^{1/2}} \left(z_s^* \frac{d\mu}{dx} + \mu \frac{dz_s^*}{dx}\right) \quad \text{on } x = x_s \tag{2.26}$$

However, the sponge function is smoothly varying and constrained to be equal to unity at $x = x_s$ thus,

$$\frac{d\mu}{dx} = 0 \quad \text{on } x = x_s \tag{2.27}$$

This gives, on substitution of equations (2.27) and (2.26) into (2.25)

$$R = \frac{ik\ z_s^* + dz_s^*/du}{ik\ z_s^* - dz_s^*/dx}\Bigg|_{x=x_s} e^{-2ikx_s} \tag{2.28}$$

Substituting for $z_s^*(x)$ from equation (2.21), and noting that $\frac{df}{dx}\Big|_{x=x_s} = -\gamma(x_s)$, from equation (2.20), gives

$$R = \left(\frac{\sinh f(x_s) - \cosh f(x_s)}{\sinh f(x_s) + \cosh f(x_s)}\right) e^{-2ikx_s} \tag{2.29}$$

where we have used $\mu(x_s) = 1$, and therefore $\gamma(x_s) = ik$ from equation (2.17).

Thus,

$$f(x_s) = \int_{x_s}^{x_e} (ik\mu - \frac{1-\mu}{C_r \Delta x})\, ds \qquad (2.30)$$

from equations (2.17) and (2.20)

$$\text{Putting } M = \int_{x_s}^{x_e} \mu(s)\, ds \qquad (2.31)$$

leads to

$$R = -e^{-2(M + x_s - x_e)/C_r\Delta x} . e^{-2ik(M+x_s)} \qquad (2.32)$$

From equation (2.31), $M \geq (x_e - x_s)$, and so equations (2.32) gives $|R| \leq 1$. Clearly, by choosing M and x_s such that $e^{-2ik(M+x_s)}$ is negative, R can be made positive. In the special case

$2k(M + x_s) = (2n + 1)\pi$ where n is an integer

we have simply

$$R = e^{-2(M + x_s - x_e)/C_r\Delta x} \qquad (2.34)$$

or

$$R = e^{\{2x_e - (2n + 1)\pi/k\}/C_r\Delta x} \qquad (2.35)$$

By careful choice of M and x_s, it is expected that the reflection coefficient of the sponge can be tuned to the desired range of values.

2.3 A particular choice of sponge function

In order to calculate M, and so the reflection coefficient as given in equation (2.35), it is necessary to choose the function $\mu(x)$. Larsen and Dancy (Ref 3) chose a complicated, but initially very gently varying function, to ensure complete absorbtion. However because we want to reflect a certain amount of energy, a simpler function may be admissible. As a first attempt, the quadratic function will be used. This allows both

$$\mu(x_s) = 1, \qquad \left.\frac{d\mu}{dx}\right|_{x = x_s} \tag{2.36}$$

as required, and by increasing or decreasing the value of $\mu(x_e)$, M can be varied, since

$$M = \int_{x_s}^{x_e} \mu(s)\ ds \tag{2.31}$$

We are free to choose $x_s = 0$, and then we can put $x_e = L$, the length of sponge. Then the function

$$\mu(x) = (N - 1)\ \frac{x^2}{L^2} + 1 \tag{2.37}$$

$$\text{gives} \qquad \mu(x_e) \equiv \mu(L) = N \tag{2.38}$$

where N can be viewed as a scaling parameter. Substituting equation (3.37) into equation (2.31) gives

$$M = (N + 2)\ \frac{L}{3} \tag{2.39}$$

so for a given length of sponge L, M is varied simply by choosing different values of N, which corresponds to the value of $\mu(x)$ at the boundary behind the sponge.

For $x_s = 0$, equation (2.32) simplifies to

$$R = -e^{-2(M-L)/C_r \Delta x} e^{-2ikM} \tag{2.40}$$

Clearly for a given wavenumber k, M can be chosen to make R real. However, this would not be true for other components of a random sea, which would have differing wavenumbers.

The sponge function $\mu(x)$ is introduced to the scheme at $(L/\Delta x)$ cells behind the boundary, increasing from $\mu = 1$ at distance L from the boundary, to the value

$$\mu = (N - 1) \frac{(L - \Delta x)^2}{L^2} + 1$$

(for equation (2.37)) one cell from the boundary. Because zero elevation is imposed at the boundary, the sponge function cannot be defined, even discretely over the last cell. This will introduce an error, which decreases with decreasing Δx.

3 RESULTS OF NUMERICAL TESTS OF THE SPONGE LAYER

3.1 Implementation of the sponge

The sponge layer was introduced to the numerical model according to equations (2.9) and (2.10). These equations are much simpler than the full two dimensional Boussinesq equations. However, it was anticipated that with the double application of the sponge (both before and after the calculation of the velocities) the linear theory would give a good indication of the nonlinear behaviour.

So far, numerical tests have been conducted with the model representing a long flume, with the input being defined at the opposite end of the flume to the sponge. The linear equations have been solved with an input sine wave, and the full Boussinesq equations have been solved with an input wave closely approximating a cnoidal wave (using the first two terms of a Stokes' expansion). All these tests have been one dimensional, although it is anticipated that obliquely incident waves will also be reflected as required using the sponge layer.

To study the response of the sponge layer to a spectrum of frequencies, the input wave period was varied from 4s to 33.3s, which was considered to represent the maximum range from a short period wave up to a set down. In all the tests, a space step of 5m and a time step of 0.7s were used. The constant depth of the flume was taken to be 5m, giving a Courant number of 0.98.

3.2 Totally absorbing sponge layer tests

It was already known that the sponge function previously used in the numerical model (see Ref 1) was effective at absorbing waves, even those of wavelengths up to at least five times the length of sponge. This older sponge function was applied once in the program, to the updated elevations and velocities prior to beginning the next interaction. It was also used with a linear radiation boundary condition, and did not prescribe the elevation at the back of the sponge.

Initial tests of the new sponge, using sponge parameters N and L such that equation (2.40) predicted very small R, indicated that the theory was accurate for input wave periods up to 10s. However, longer period waves were partially reflected. Therefore, further tests were made using the new quadratic sponge function, as described in Chapter 2, but with the single sponge application linked to a radiation boundary condition. It was found that this successfully absorbed waves much larger than the sponge layer. As an example, a four cell sponge (L = 20m) with N = 1.833 caused negligible reflection of a 33.3m period wave, with wavelength of 233.3m. Tests of a wave generated using the first two terms of a Stokes' expansion of a cnoidal wave (referred to later simply as a cnoidal wave) indicated that nonlinear waves were also absorbed well.

3.3 Partially reflecting sponge layer tests

First attempts to control the reflection behaviour of the sponge, showed that for a 10s period input wave, it was necessary to use less than ten cells of sponge to get the required behaviour. Using many cells of sponge absorbed more of the wave than predicted by the theory. This is an unimportant restriction, because in practice we prefer to minimise the number of cells in the scheme covered by the sponge layer.

Initial calculations of R from equation (2.40), with the choice

$$2kM = (2n + 1)\pi \qquad (3.1)$$

in order to give real, positive R, showed this to be a severe restriction on the choice of R. For example, consider a 10 cell sponge with $\Delta x = 5$m, so that $L = 50$m. With a 10s period wave in 5m of water, the wavelength $\lambda = 70$m. Also, we can rewrite equation (3.1) as

$$M = \frac{(2n + 1)}{4} \lambda \qquad (3.2)$$

Hence, $n = 0$ gives $M = 17.5$, which is inadmissible because it is less than L (consider equation (2.40) - this gives $|R| = e^{-2(M-L)/C_r \Delta x}$). The next value of M which gives real, positive R is for $n = 1$, and is $M = 52.5$. This gives

$$R = e^{-1} = 0.368 \qquad (3.3)$$

All higher values of n give very small R. Therefore there is only one useful choice of M which satisfies equation (3.2), which is very limiting. In addition, in a random sea, only the 10s period component will respond to the sponge layer in this way. Therefore, all the tests carried out were to investigate the more practical use of a complex theoretical reflection coefficient, as the viability of the sponge layer depends on good performance under these conditions.

3.3.1 Linear input waves

For a given length of sponge and period, equation (2.40) gives the theoretical variation of R with M, where M is directly proportional to N (equation 2.39)). In Figure 1 the modulus of R is shown plotted against a parameter ϵ, where

$$\epsilon = M - L \qquad (3.4)$$

which gives

$$N = 3\frac{(L + \epsilon)}{L} - 2 \qquad (3.5)$$

Clearly $\epsilon = 0$ gives total reflection, and as ϵ increases the theoretical reflection coefficient reduces. Figure 1 is for 4 cells of sponge and a 10s period. As in all tests $\Delta x = 5$m and the water depth is also 5m.

To test the theory, numerical tests were made using 4 cells of sponge and an input sine wave of 10s period, for various values of ϵ. The results of these tests are tabulated in Table 1, and plotted as linear numerical results in Figure 1. As can be seen, the agreement with the theoretical $|R|$ is good for $R \geq 0.3$, ie $\epsilon \leq 3$. For larger values of ϵ, it appears that the minimum reflection coefficient achieved is about 0.2. It is not surprising that a sponge layer only 20m long cannot achieve $R \leq 0.2$ for a 70m wave, and indeed it is likely that for large ϵ, corresponding to a steeply changing sponge, R will increase again. The failure of the theory to predict the numerical results for large values of ϵ can be attributed to the approximations made, as detailed in section 2.2.

All the reflection coefficients deduced from numerical results were calculated using a method described in the Appendix. This method is based on assuming the motion is due to two sine waves travelling in opposite directions, different only in phase and amplitude. Spectral analysis was inappropriate here, as the record length was too short. More data could not easily be obtained, as this would required running the model with a greater number of timesteps with the consequent risk of secondary reflections from the paddle contaminating the solution. It was necessary to calculate R from elevations calculated before a secondary reflection began to influence them.

The results for a period of 10s, shown in Figure 1, were encouraging, but for practical applications it is important that given sponge layer characteristics (N,L) will behave as predicted for other periods. Therefore, a similar series of tests were run for a 4s period, and the resulting reflection coefficients are compared with the theoretical values in Figure 2. Again, the agreement with the theorectical $|R|$ is good, and as could be expected for this 20m wavelength, a lower reflection coefficient, less than 0.1, is achieved. The results are also given in Table 2. The highest ϵ numerical result in this case, $\epsilon = 9$, suggests that there may be an increase in R for larger ϵ.

Further results showing a comparison between numerical and theoretical reflection coefficient, for a range of input wave periods, are shown in Table 3.

In an attempt to make a comparison between the numerical results and experimental reflection results, the response of the numerical model with a sponge layer 4 cells long and with $\epsilon = 5$ (or $N = 1.75$) was tested. These results are all contained in Table 1, 2 or 3, and plotted on the same graph as some experimental results in Figure 3. The experimental results are for a rip-rap (16 to 20 tonnes with a specific gravity of 2.7) placed at four different slopes. It can be seen that the sponge layer 4 cells wide with $\epsilon = 5$ approximate the 1:3 slope experimental results quite well. (Note that the time scaling is approximately 1:8, so that the frequency 1 Hz as shown scaled to 1/8 Hz.)

To illustrate the behaviour of the sponge layer, profiles of the elevation in the flume are shown in Figures 4 and 5, for the case of a 7.5s period input wave, and a sponge layer 4 cells wide with $\epsilon = 1.6$ ($N = 1.24$). In Figure 4, the profile after 60.9s (87 time steps) is shown, and it is clear that the first reflected wave has returned to nearly half way down the flume, and that the two waves are interfering constructively. In Figure 5, the profile three time steps (2.1s) later is shown, when the waves are interfering destructively.

3.3.2 Nonlinear input waves

To study the response of the sponge layer when solving the Boussinesq equations in one dimension, a cnoidal wave was input at the paddle. Three cases were run, all with a period of 10s and amplitude of 0.1m, but with three values of ϵ for the sponge layer: $\epsilon = 0.5$, 1.6 and 2.5. Calculation of the reflection coefficient for a cnoidal wave cannot be achieved as described in the Appendix for the linear case. Instead, the flume length was doubled from approximately 300m to nearly 600m, in order to calculate elevations over 128 time steps at several positions in the flume. The elevations were then spectrally analysed and the results are shown in Table 4. The maximum and minimum amplitudes of the positions analysed, at the fundamental frequency and first harmonic, and for each value of ϵ are shown. The reflection coefficient has been calculated in each case using the equation

$$R' = \frac{H_{max} - H_{min}}{H_{max} + H_{min}} \qquad (3.6)$$

There are two obvious inaccuracies in this calculation: equation (3.6) is derived assuming the motion is due to a sine wave and its sine wave reflection, which is not the case here; also, equation (3.6) requires H_{max} to be the antinode and H_{min} the node of the motion, which is very unlikely to be true of any of the positions in the flume chosen for analysis. These inaccuracies will result in an underestimate of R, and this would appear to be true of the calculated reflection coefficient shown in Table 4.

The three calculated reflection coefficients for the fundamental frequency, are shown in Figure 1 as the nonlinear fundamental frequency numerical results. Bearing in mind the likely errors, they are close to the theoretical values. The calculated reflection coefficients of the first harmonic are less close to the theoretical value. However, due to the lack of experimental data, it is not known what reflection characteristics can be expected of a cnoidal wave.

To illustrate the performance of the sponge layer with an incident cnoidal wave, Figure 6 shows the profile in a short flume of a 10s period wave, after 75.6s (108 time steps). The sponge layer is 4 cells long, with $\epsilon = 1.6$ ($N = 1.24$).

4 CONCLUSIONS AND RECOMMENDATIONS

4.1 Conclusions

1. The theory of sponge layers has been developed to allow their use in representing partially reflecting boundaries in the numerical model.

2. The sponge layer theory allows it to be tuned to give the required reflection coefficient at a specified frequency. For a given set of sponge

layer parameters, its behaviour across the frequency range has been shown to compare favourably with physical model results.

3. In addition to representing partially reflecting boundaries, the sponge layer approach can also be used for totally absorbing boundaries. This makes it a more flexible boundary condition than many of the others which have been considered.

4. The sponge layer has been shown to respond well both to linear and non-linear waves.

4.2 Recommendations

1. All the tests described here have been for the one dimensional case. Further work will therefore be required to ensure the sponge layer will reflect obliquely incident waves as desired. This will require careful consideration of the transverse and horizontal velocity flags in setting up the model.

2. Further tests are also required to examine the sensitivity of the sponge layer to variations in some of its parameters, these include:

   (i) The effect of changes to Δx and Δt; it is likely that decreasing these values will improve agreement with the theoretical reflection coefficient.

   (ii) Examining the behaviour of the sponge for $\epsilon < < 1$ and $\epsilon > 10$. Very small ϵ values may lead to instabilities because of the imposition of zero elevation behind the sponge. Large ϵ will probably increase the reflection coefficient, thus allowing values closer to unity to be represented more readily.

(iii) Variation in the width of sponge this should demonstrate that most physically occurring boundaries in a harbour can be accurately represented.

3. To fully validate this method of representing boundaries comparisons will need to be made with the results from a physical model.

5 ACKNOWLEDGEMENTS

The research described in this report was carried out by members of Dr S W Huntington's Maritime Engineering Department. The authors would like to thank colleagues in the department for their helpful discussions. In particular, acknowledgement is due to Dr E C Bowers for his help and advice.

6 REFERENCES

1. Smallman J V, Matsoukis P C, Cooper A J and Bowers E C. The Development of a Numerical Model for the Solution of the Boussinesq Equations for Shallow Water Waves - Constant Depth Case. Hydraulics Research Report No SR 137, August 1987.

2. Jones D V and Smallman J V. The Development of a Numerical Model for the Solution of the Boussinesq Equations for Shallow Water Waves. Variable Depth Case. Hydraulics Research Report No SR 159. February 1988.

3. Larsen J and Dancy H. Open Boundaries in Short Wave Simulations - A New Approach. Coastal Engineering, 7 No 3, 285-297. 1983.

4. Israeli M and Orszag S A. Approximation of Radiation Boundary Conditions. J Comp Physics 41 115-135, (1981).

5. Chubarov L B and Shokin Y I. The Numerical Modelling of Long Wave Propagation in the Framework of Non-linear Dispersion Models. Computers and Fluids 15 No 3, 229-249. 19

6. Burgess N A. Stable Boundary Conditions for the Shallow Water Equations. Phd thesis, Oxford University. September 1987.

7. Liao Z P and Wong H L. A transmitting boundary for the numerical simulation of elastic wave propagation. Soil Dynamics and Earthquake Engineering, 3 No 4, 174-183. 1984.

8. Madsen P A. Wave Reflection From a Vertical Permeable Wave Absorber. Coastal Engineering, 7, 381-396. 1983.

9. Bear J. Dynamics of fluids in porous media. Elsevier Publishing Company. 1975.

10. Berkhoff J C W. Mathematical models for simple harmonic linear water waves. Wave diffraction and refraction. Delft Hydraulics Laboratory Report. 1976.

TABLES.

TABLE 1 Sponge layer (4 cells) results with an input sine wave of period T = 10s

N	ϵ	Theoretical $\|R\|$	Approximate Numerical $\|R\|$
1.092	0.61	0.78	0.77
1.129	0.86	0.70	0.69
1.184	1.23	0.60	0.59
1.240	1.60	0.52	0.49
1.375	2.50	0.36	0.37
1.525	3.50	0.24	0.28
1.750	5.00	0.13	0.22
2.050	7.00	0.06	0.20

TABLE 2 **Sponge layer (4 cells) results with an input sine wave of period $T = 10s$**

N	ϵ	Theoretical $\lvert R \rvert$	Approximate Numerical $\lvert R \rvert$
1.075	0.50	0.82	0.79
1.240	1.60	0.52	0.45
1.375	2.50	0.36	0.29
1.525	3.50	0.24	0.18
1.750	5.00	0.13	0.09
2.050	7.00	0.06	0.05
3.35	9.00	0.002	0.07

TABLE 3 **Further sponge layer results with an input sine wave and various periods**

In all these tests, 4 cells of sponge were used

Period	N	ϵ	Theoretical $\lvert R \rvert$	Approximate Numerical $\lvert R \rvert$
5	1.24	1.6	0.52	0.44
6	1.75	5.0	0.13	0.06
7.5	1.24	1.6	0.52	0.46
7.5	1.75	5.0	0.13	0.12
13.3	1.75	5.0	0.13	0.37
20	1.24	1.6	0.52	0.61
20	1.75	5.0	0.13	0.46
33.3	1.24	1.6	0.52	0.66

TABLE 4 Sponge layer results with an input cnoidal wave, of period 10s

The cnoidal wave was approximated by the first two terms of its Stokes' expansion. The amplitude of the first term was 0.1m.

N	ϵ	Fundamental Spectral component 0.1Hz	1st harmonic Spectral component 0.2Hz	Expected value R f=0.1Hz	R f=0.2Hz
1.075	0.5	H_{max} : 0.173m H_{min} : 0.024m	H_{max} : 0.021m H_{min} : 0.008m	0.76	0.42
1.240	1.6	H_{max} : 0.142m H_{min} : 0.058m	H_{max} : 0.012m H_{min} : 0.004m	0.42	0.50
1.375	2.5	H_{max} : 0.127m H_{min} : 0.074m	H_{max} : 0.009m H_{min} : 0.005m	0.26	0.35

Notes: (i) A series of consecutive flume positions were used to collect data, which was spectrally analysed. Therefore the H_{max} and H_{min} values are only exact, if two of the positions correspond with an antinode and node respectively.

(ii) The 'spectral component' 0.1Hz corresponds to the fundamental frequency of the cnoidal wave. The 0.2Hz component is the first harmonic.

(iii) The reflection coefficients were calculated using the expression derived using linear theory:

$$R = (H_{max} - H_{min}) / (H_{max} + H_{min})$$

FIGURES.

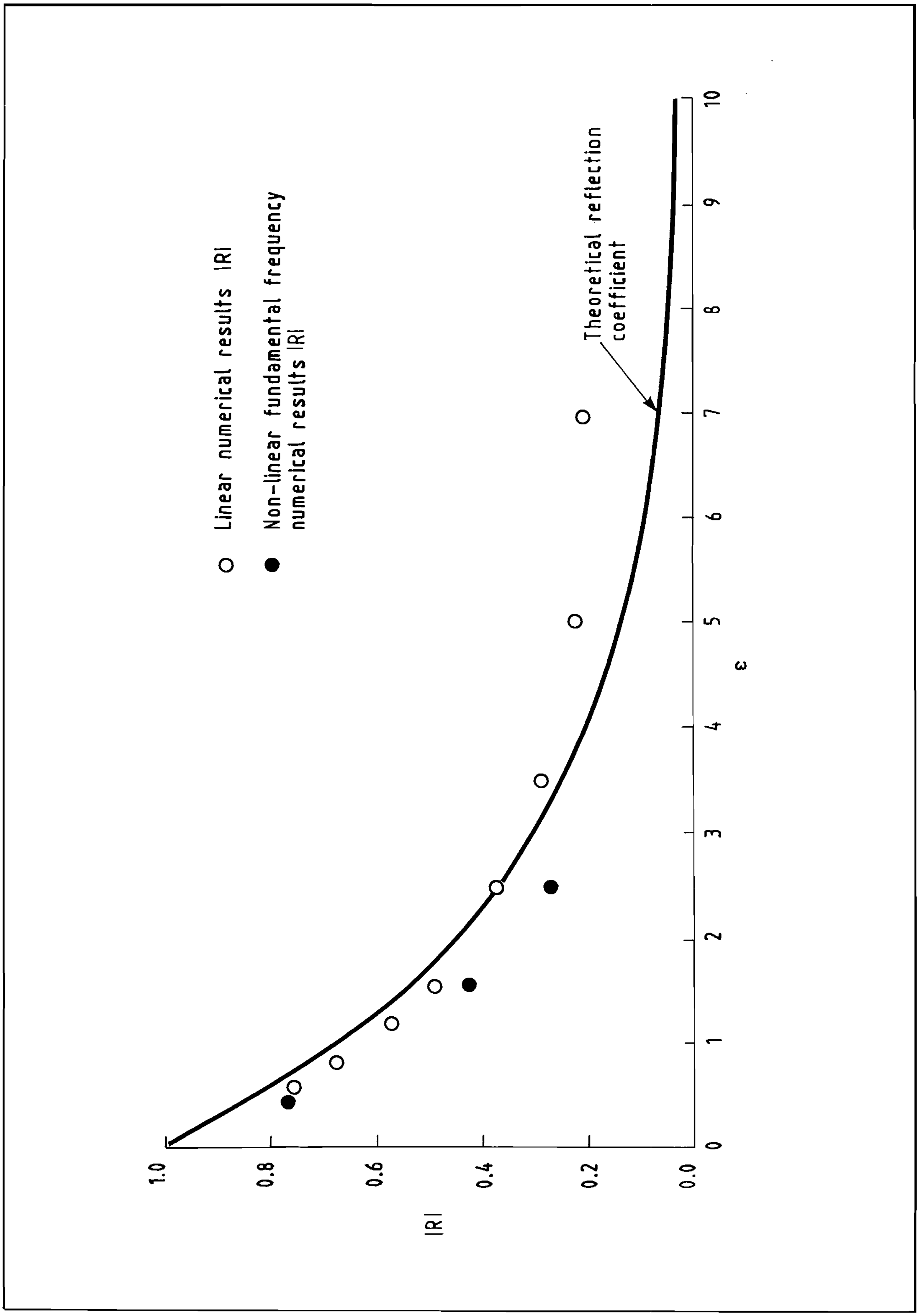

Fig 1 Comparison of theoretical reflection coefficient with numerical results for a 10s period wave

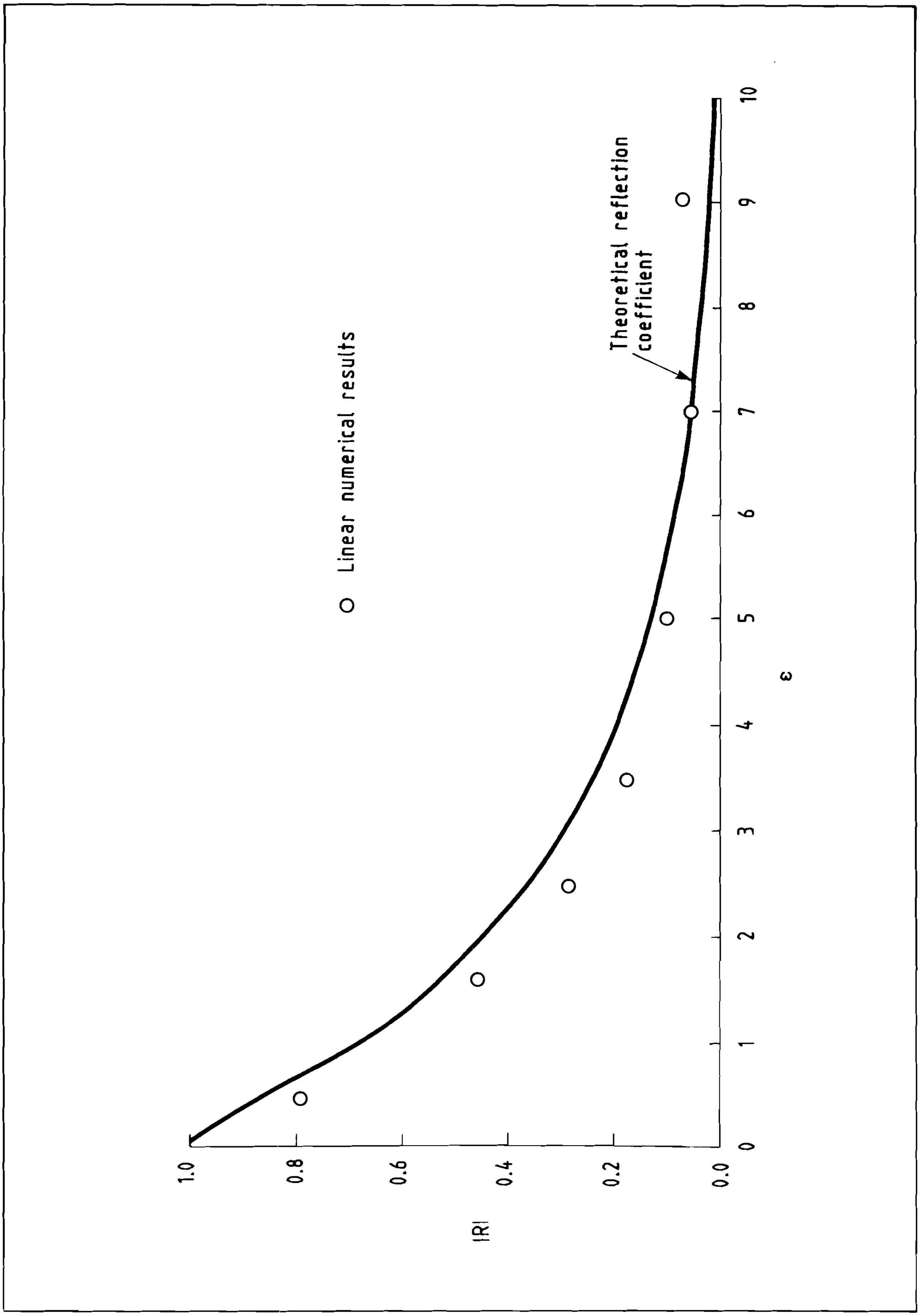

Fig 2 Comparison of theoretical reflection coefficient with numerical results for 4s period wave

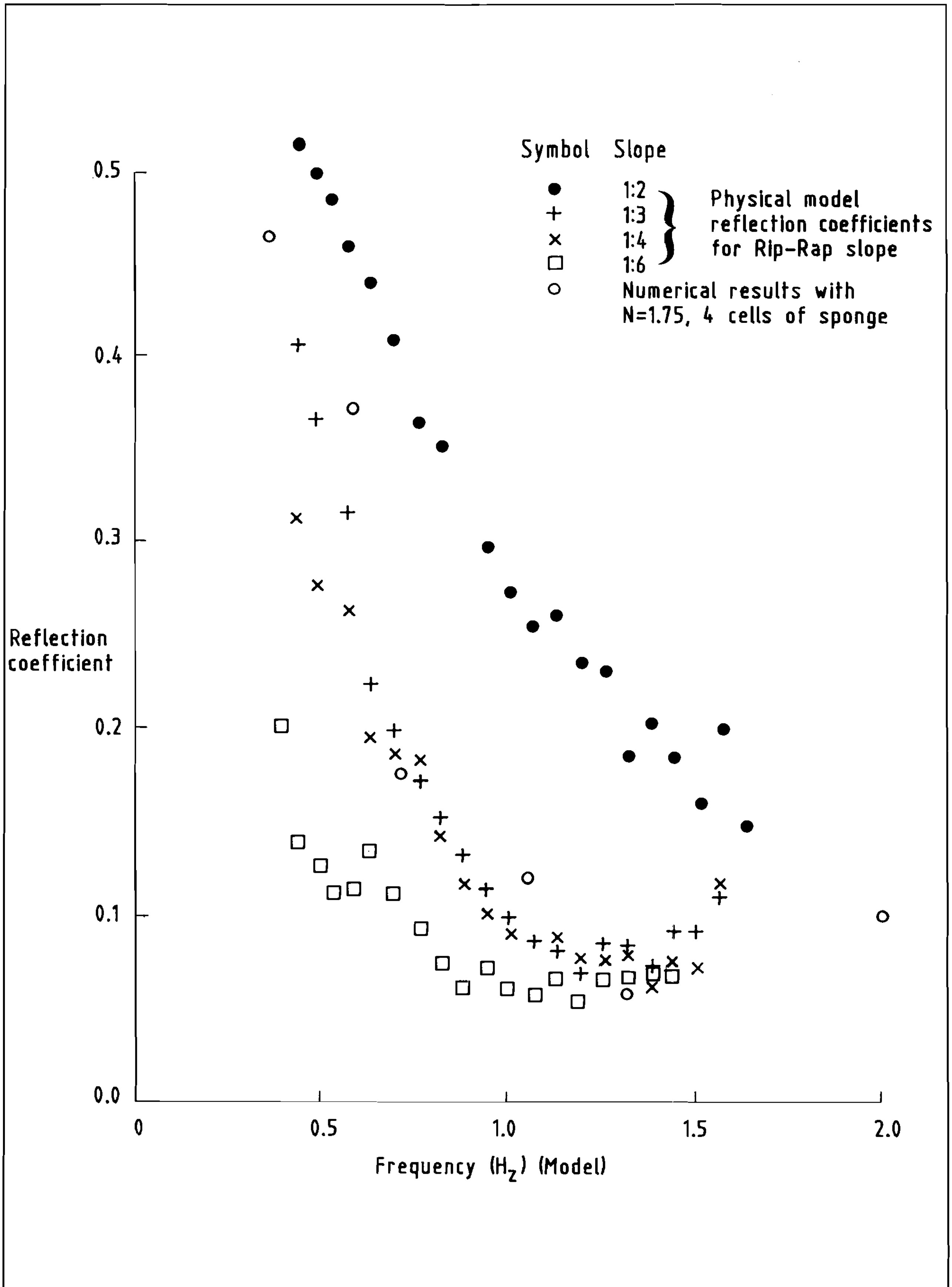

Fig 3 Comparison of numerical model results with physical model reflections coefficients

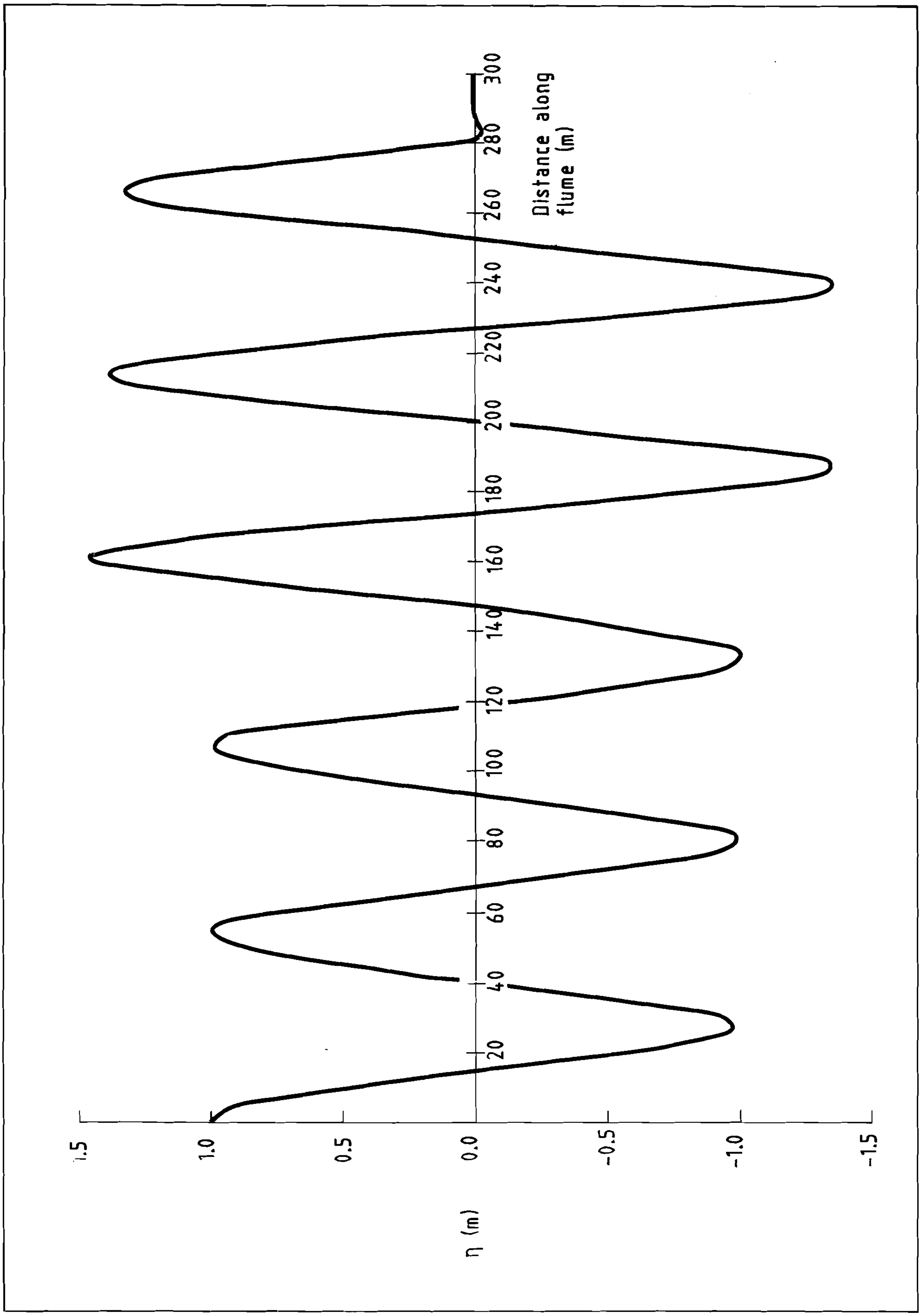

Fig 4 Profile of wave elevation for a 7.5s period after 60.9s

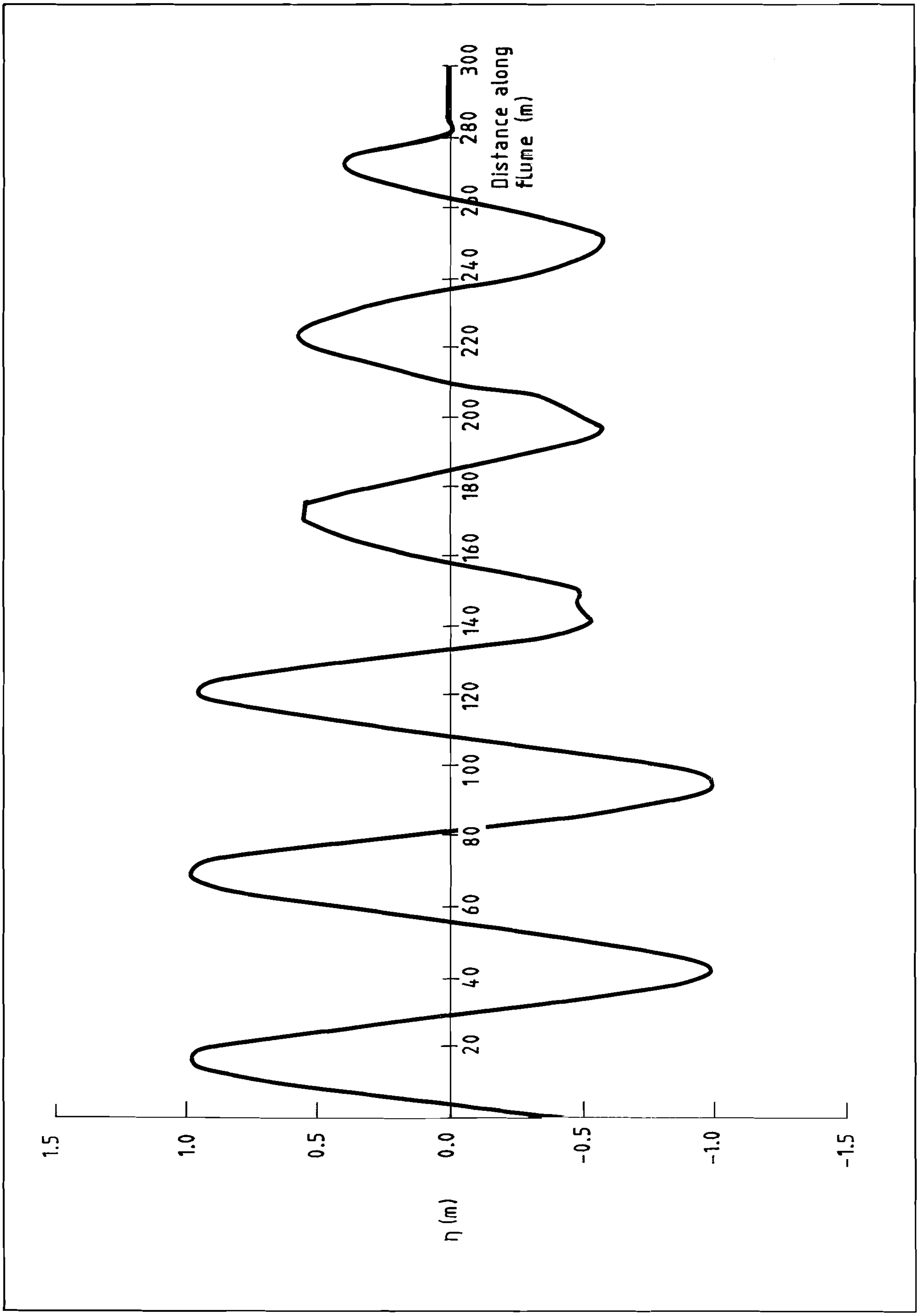

Fig 5 Profile of wave elevation for a 7.5s period wave after 63s

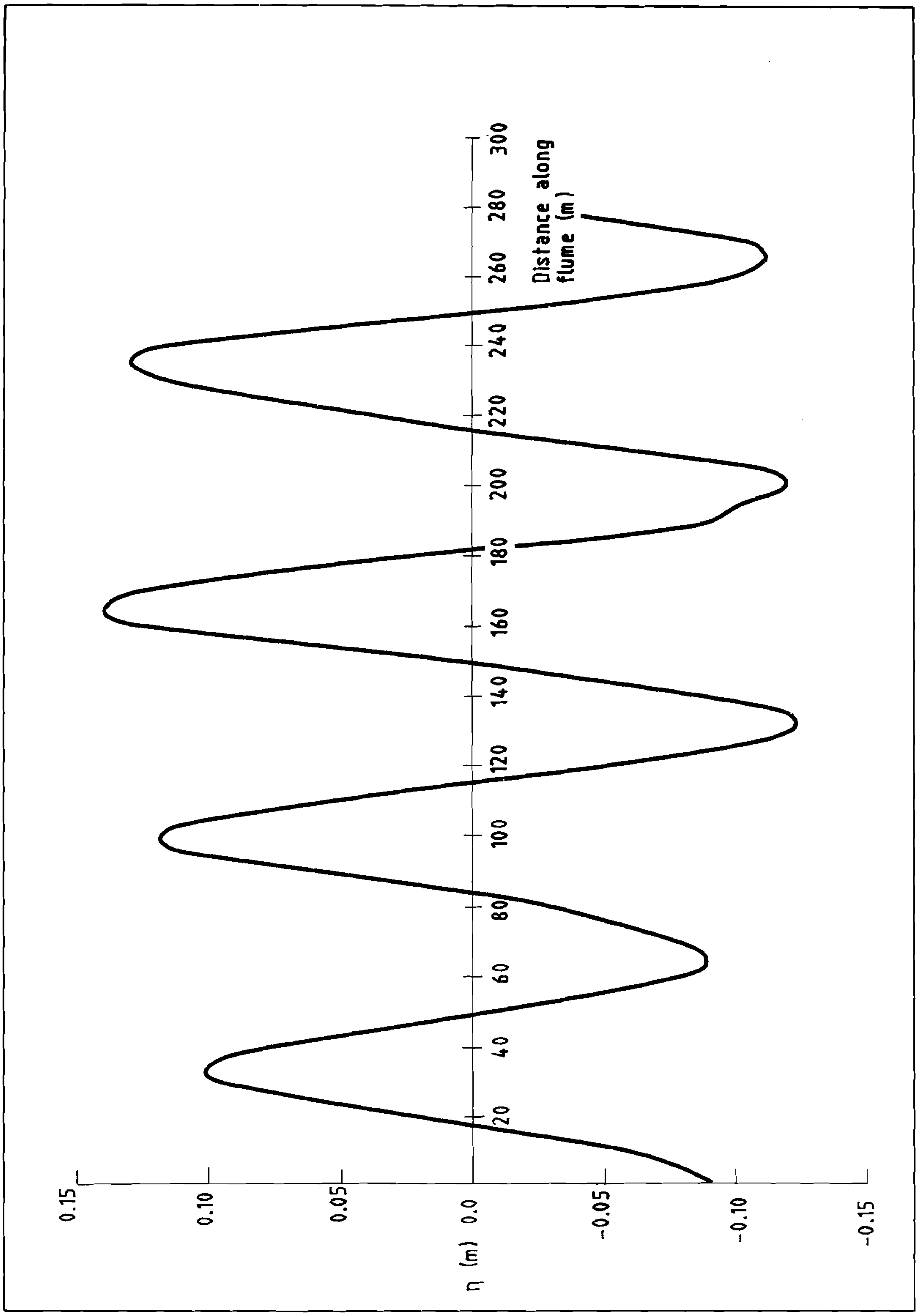

Fig 6. Profile of wave elevation for 10s period cnoidal wave after 75.6s

APPENDIX.

APPENDIX

Calculation of reflection coefficient for a sine wave

The wave profile due to an input sine wave and its reflection, where the reflection coefficient is R, may be written

$$\eta = A\cos\,(wt - kx) + R\,A\cos\,(wt + kx + \phi) \qquad (A.1)$$

Here, A, w and k are known from the input wave conditions. Now if a and b are the elevations at two positions x and $(x + \Delta x)$, at time t, and c and d are the elevation at x and $(x + \Delta x)$ but at time $(t + \Delta t)$, we can write

$$a = A\cos\,(wt - kx) + AR\cos\,(wt + kx + \phi) \qquad (A.2)$$

$$b = A\cos\,(wt-k(x+\Delta x)) + AR\cos\,(wt+k(x+\Delta x)+\phi) \qquad (A.3)$$

$$c = A\cos\,(w(t+\Delta t)-kx) + AR\cos\,(w(t+\Delta t)+kx+\phi) \qquad (A.4)$$

$$d = A\cos\,(w(t+\Delta t)-k(x+\Delta x))+AR\cos\,(w(t+\Delta t)+k(x+\Delta x)+\phi) \qquad (A.5)$$

Using trigonometrical identities, and for convenience putting A = 1, equations (A.3) and (A.2) give

$$b = a\cos k\Delta x + \sin k\Delta x\,(\sin(wt-kx) - R\sin\,(wt+kx+\phi) \qquad (A.6)$$

Equations (A.4) and (A.2) give:

$$c = a\cos w\Delta t - \sin w\Delta t\,(\sin(wt-kx) + R\sin\,(wt+kx+\phi)) \qquad (A.7)$$

Equations (A.5) and (A.2) give:

$$d = \sin w\Delta t \sin k\Delta x \,(a - 2R\cos (wt+kx+\phi) + c \cos k\Delta x + \cos w\Delta t \,(b - a \cos k\Delta x) \qquad (A.8)$$

Manipulation of equations (A.2), (A.6), (A.7) and (A.8) to eliminate x,t and O finally gives

$$R = \frac{\left\{ \begin{array}{c} a^2+b^2+c^2+d^2+2ad \cos(w\Delta t+k\Delta x) + 2bc \cos(w\Delta t-k\Delta x) \\ -2(ac+bd) \cos w\Delta t - 2(ab + cd) \cos k\Delta x \end{array} \right\}^{1/2}}{2 \sin k\Delta x \sin w\Delta t}$$

Hence, given the elevations at adjacent cells for consecutive time steps, the reflection coefficient for the case of a sine wave and its reflection can be calculated.